Am J Physiol Lung Cell Mol Physiol 300: L624–L632, 2011.
First published January 14, 2011; doi:10.1152/ajplung.00376.2010.

LPS-induced decrease in intracellular labile zinc, $[Zn]_i$, contributes to apoptosis in cultured sheep pulmonary artery endothelial cells

Kalidasan Thambiayya, Karla J. Wasserloos, Zhentai Huang, Valerian E. Kagan, Claudette M. St. Croix, and Bruce R. Pitt

Departments of Bioengineering and Environmental and Occupational Health, University of Pittsburgh and University of Pittsburgh Graduate School of Public Health, Pittsburgh, Pennsylvania

Submitted 22 October 2010; accepted in final form 11 January 2011

Thambiayya K, Wasserloos KJ, Huang Z, Kagan VE, St. Croix CM, Pitt BR. LPS-induced decrease in intracellular labile zinc, $[Zn]_i$, contributes to apoptosis in cultured sheep pulmonary artery endothelial cells. *Am J Physiol Lung Cell Mol Physiol* 300: L624–L632, 2011. First published January 14, 2011; doi:10.1152/ajplung.00376.2010.—A role in signal transduction for a vanishingly small labile pool of intracellular zinc ($[Zn]_i$) has been inferred by the sensitivity of various physiological pathways to zinc chelators such as N,N,N′,N′-tetrakis(2-pyridylmethyl) ethylenediamine (TPEN) and/or associations with changes in nonprotein-bound zinc-sensitive fluorophores. Although we (44) reported that LPS-induced apoptosis in cultured sheep pulmonary artery endothelial cells (SPAEC) was exacerbated by TPEN, *1*) we did not detect acute (30 min) changes in $[Zn]_i$, and *2*) it is unclear from other reports whether LPS increases or decreases $[Zn]_i$ and whether elevations or decreases in $[Zn]_i$ are associated with cell death and/or apoptosis. In the present study, we used both chemical (FluoZin-3 via live cell epifluorescence microscopy and fluorescence-activated cell sorting) and genetic (luciferase activity of a chimeric reporter encoding zinc-sensitive metal-response element and changes in steady-state mRNA of zinc importer, SLC39A14 or ZIP14) techniques to show that LPS caused a delayed time-dependent (2–4 h) decrease in $[Zn]_i$ in SPAEC. A contributory role of decreases in $[Zn]_i$ in LPS-induced apoptosis (as determined by caspase-3/7 activation, annexin-V binding, and cytochrome *c* release) in SPAECs was revealed by mimicking the effect of LPS with the zinc chelator, TPEN, and inhibiting LPS- (or TPEN)-induced apoptosis with exogenous zinc. Collectively, these are the first data demonstrating a signaling role for decrease in $[Zn]_i$ in pulmonary endothelial cells and suggest that endogenous levels of labile zinc may affect sensitivity of pulmonary endothelium to the important and complex proapoptotic stimulus of LPS.

pulmonary endothelium; lipopolysaccharide

INTRACELLULAR ZINC ($[Zn]_i$) is maintained within a narrow range (100 to 500 μM) across numerous cell types and species by the coordinate activity of a large family of Zn importers (SLC39A1–14 or ZIP1–14) and transporters (SLC30A1–10 or ZnT1–10), intracellular storage vesicles, and Zn-binding proteins (12, 17). Like iron (and other divalent cationic metals), it is considered a trace element because its labile concentration is vanishingly small with estimates between 10^{-9} M (11, 33) to 10^{-12} M (7). Depending on the species, zinc is associated with 3–10% of the genome (1) and in humans is an essential component of more than 300 enzymes, 2,000 transcription factors, and a large number of receptors, cytoskeletal proteins, and other potential regulatory targets (8). As such, the labile pool of $[Zn]_i$ has been considered in the context of intracellular signal transduction including pathways of cell growth, death and differentiation and inflammation, as well as contraction and secretion. Although difficult to quantify, this labile pool is operationally defined as the intracellular zinc compartment chelated by molecules such as N,N,N′,N′-tetrakis(2-pyridylmethyl)ethylenediamine (TPEN) and/or detected by nonprotein-bound zinc-sensitive fluorophores (including FluoZin-3).

In contrast to the role of zinc in the central nervous, immune, reproductive, gastrointestinal, and/or endocrine systems, considerably less is known about zinc in the lung. It is noteworthy that zinc deficiency (via dietary manipulations) in experimental animals exacerbates lung injury secondary to hyperoxia (46), cecal ligation and puncture (31) and alcohol (26). In an analogous fashion to calcium, however, most studies assessing a role for $[Zn]_i$ in pulmonary endothelium (and other organs and cell types) have focused on transient elevations in $[Zn]_i$ and associations with peroxide-induced cell death (44, 52) and contraction (5). A recent report (30), however, noted for the first time that a decrease in $[Zn]_i$ may be a critical signaling component in the context of LPS-induced maturation of cultured mouse dendritic cells. We (44) noted that TPEN caused a dose-dependent increase in spontaneous apoptosis in pulmonary endothelium and that TPEN exacerbated LPS-induced apoptosis in cultured sheep pulmonary artery endothelial cells (SPAEC), a phenomenon noted by others (7) in cytokine and lipid-induced apoptosis in cultured systemic endothelium. Nonetheless, in our original study (44), we were not able to detect LPS-induced acute (30 min) changes in $[Zn]_i$. Others (20) have reported that LPS actually acutely increases $[Zn]_i$ in human leukocytes and that hydrogen peroxide-induced increases in $[Zn]_i$ are associated with apoptosis in fetal SPAEC (51). Accordingly, we sought to determine whether LPS-induced changes in $[Zn]_i$ occurred somewhat later (2–4 h) after exposure of SPAEC to a proapoptotic stimulus of LPS (23–25) and whether changes in $[Zn]_i$ were necessary and sufficient to mediate LPS-induced apoptosis in SPAEC. As decreases in trace metals can be subtle and subject to artifact, we utilized multiple chemical (live cell fluorescence; fluorescence-activated cell sorting, FACS) and genetic [chimeric reporter-encoding zinc-sensitive region of metal-responsive element (MRE) fused to luciferase; steady-state mRNA levels of ZIP14] detection systems. The ability of TPEN to mimic the effect of LPS-induced apoptosis and rescue of LPS phenotype with exogenous zinc is consistent with a central role for decreases in $[Zn]_i$ and LPS-induced apoptosis in SPAEC.

Address for reprint requests and other correspondence: B. Pitt, Bridgeside Point Bldg., 100 Technology Dr., Suite 555, Pittsburgh, PA 15219 (e-mail: brucep@pitt.edu).

MATERIALS AND METHODS

Isolation and culture of SPAECs. SPAECs were cultured from sheep pulmonary arteries obtained from a nearby slaughterhouse as previously described (24). Early passage cells were sorted to homogeneity on the basis of uptake of fluorescence-labeled 1,1′-dioctadecyl-3,3,3′,3′-tetramethylindocarbocyanine-labeled acetylated low-density lipoprotein and subcultures were routinely monitored for platelet endothelial cell adhesion molecules (CD31) expression to assure endothelial phenotype and purity. The SPAECs were grown in OptiMEM (GIBCO, Grand Island, NY) supplemented with 10% fetal bovine serum, 100 U/ml penicillin, and 100 μg/ml streptomycin at 37°C in an atmosphere with 5% CO_2.

Treatments. Zinc, TPEN, pyrithione, and LPS solutions were prepared fresh from zinc chloride, TPEN, mercaptopyridine N-oxide sodium salt, and *Escherichia coli 0111:B4*, respectively (Sigma-Aldrich, St. Louis, MO).

Fluorescence microscopy. SPAECs were cultured on Lab-Tek-chambered 1.0 borosilicate coverglass slides (Naperville, IL). Cells were exposed to LPS (100 ng/ml in each well per time point, 0.5 to 4.0 h) or TPEN (2 μM, 4 h). After treatment, cells were washed (2×) with HBSS (Ca^{2+}/Mg^{2+}) and incubated (37°C; 20 min) with 2–5 μM FluoZin-3 AM (Molecular Probes, Eugene, OR) and equal volume of Pluronic F-127 (Invitrogen, Carlsbad, CA) in HBSS (Ca^{2+}/Mg^{2+}). Subsequently, cells were washed (2×) with HBSS (Ca^{2+}/Mg^{2+}) and immediately imaged in the presence of HBSS (Ca^{2+}/Mg^{2+}) for each time point. All recordings were performed at room temperature (20–25°C). Cells were imaged using a Nikon TE2000E equipped with a ×40 1.3 NA oil-immersion objective, Lambda DG4 wavelength switcher, and xenon light source (Sutter Instrument, Novato, CA), charge-couple device camera (Cool-SNAP HQ; Photometrics, Tucson, AZ), and NIS-Elements software (Nikon, Melville, NY). FluoZin-3 was excited at 488 nm, and emission was detected using a 505–550-nm bandpass filter. Cells were randomly selected for each time point (0.5–4.0 h), and the mean fluorescence intensity (MFI) was quantified from the region of interest of all randomly selected cells per time point. Background subtraction was performed on all images before quantitation.

Flow cytometry. Quantification of relative changes in $[Zn]_i$ was also performed via flow cytometry (9). SPAECs were incubated (37°C; 20 min) with 2–5 μM FluoZin-3 AM ester (Molecular Probes) with Pluronic F-127 (equal volume) (Invitrogen) in HBSS (Ca^{2+}/Mg^{2+}) (Invitrogen). LPS-treated cells were rinsed in PBS, trypsinized, and centrifuged at 1,500 revolution/min for 5 min. The cell pellet was resuspended with PBS containing 100 μg/ml propidium iodide (PI) and incubated (37°C; 15 min) in the dark. In a separate series of experiments, phosphatidylserine (PS) externalization was determined with an annexin-V-FITC apoptosis detection kit (Biovision, Mountain View, CA). LPS-treated cells were rinsed in PBS, trypsinized, and centrifuged at 1,500 revolution/min for 5 min. The cell pellet was resuspended in 300 μl binding buffer and supplemented with 3 μl of FITC-annexin-V and 3 μl of PI and incubated (room temperature; 15 min) in the dark. In some experiments, cells were treated with pan-caspase inhibitor Z-Val-Ala-Asp-fluoromethylketon (Z-VAD-FMK) (Calbiochem, Gibbstown, NJ) at 30 μM for 1 h and then treated with LPS (100 ng/ml) or buffer (control). Flow cytometric analysis was performed using a FACSCanto (BD Biosciences, San Jose, CA). For each sample 10,000 events were recorded and analyzed.

Transient transfections and luciferase assays. SPAECs (80–90% confluence) were transfected with 0.6 μg of a luciferase reporter construct driven by four MRE tandem repeats (pLuc-MCS/MRE) and 0.15 μg of pSVβ-galactosidase containing *E. coli* lacZ gene reporter construct (Promega, Madison, WI) using lipofectamine and PLUS reagents (Invitrogen) (9). Cells were lysed, and luciferase assay was performed using the Luciferase Assay System (Promega). Relative light units were determined in a TD-20/20 luminometer (Turner Designs, Sunnyvale, CA). β-Galactosidase assay was performed using β-galactosidase Enzymes Assay System (Promega). Absorbance was read at 420 nm with a plate reader (Perkin-Elmer, Waltham, MA). Results were expressed as a ratio of firefly luciferase activity to β-galactosidase activity.

Accumulation of cytochrome c in cytosol. Translocation of cytochrome *c* (cyt *c*) was examined by Western blot. After LPS (100 ng/ml) treatment, SPAECs were harvested and resuspended in lysis buffer containing 250 mM sucrose, 20 mM HEPES-potassium hydroxide (pH 7.5), 10 mM potassium chloride, 1.5 mM magnesium chloride, 1 mM EDTA, 1 mM EGTA, 1 mM dithiothrestol, 1 mM PMSF, 1 mg/ml aprotinin, 1 mg/ml leupeptin, and 0.05% digitonin for 3 min on ice, then centrifuged at 8,500 *g* for 5 min. The resulting cytosolic supernatants were subjected to 12% SDS-PAGE and transferred to a nitrocellulose membrane that was probed with mouse antibodies against cyt *c* (BD Pharmingen, San Diego, CA) or β-actin (Sigma-Aldrich), followed by horseradish peroxidase-coupled detection.

Caspase-3/7 assay. SPAECs were seeded on a 96-well (BD Falcon, white/clear bottom) plate. After treatment, cells were incubated (room temperature; 1 h) with luminescence Caspase-Glo 3/7 substrate (Promega). Luminescence was measured using a plate reader (Perkin-Elmer).

Viability assay. In addition to FACS analysis of PI, viability of SPAECs was determined by quantifying reduction of a fluorogenic indicator Alamar Blue (Biosource, Camarillo, CA). Oxidized Alamar Blue is taken up by cells and reduced by intracellular dehydrogenases, and the water-soluble changes in fluorescence emission (590 nm) are utilized as an index of viability (44).

RNA isolation and real-time RT-PCR. Total RNA was isolated using RNAqueous-4PCR Kit (Ambion, Austin, TX) from untreated and treated SPAECs and DNase I (Ambion) treated to remove genomic DNA contamination and quantified by measuring absorbance (260 nm). Total RNA was reverse transcribed using iScript (BioRad, Hercules, CA) according to manufacturer's instructions. The cDNA was amplified by real-time PCR using TaqMan Gene Expression Assays (Applied Biosystems, Foster City, CA).

Primer design and PCR amplification efficiency. For most zinc importers and transporters, gene ovine sequences are not available, but these genes are conserved across bovine and human species (13). Bovine zinc importers and transporters gene sequences were blasted against the ovine genome using ovine genome browser version 1.0 (www.livestockgenomics.csiro.au), and primers were designed from bovine sequence (on the basis of conserved regions) using PrimeTime qPCR (IDT DNA Technologies, Coralville, IA). Housekeeping primers were designed from ovine glucose-6-phosphate dehydrogenase (G6PD) sequence (NCBI database) using PrimeTime qPCR (IDT DNA technologies). Amplification efficiency (E) was calculated for each gene from the slope of the dependence of amplification cycle vs. RNA concentration after running serial dilutions of RNA using the formula $E = [10^{(-1/\text{slope})} - 1] \times 100$.

Statistical analysis. Data are expressed as means ± SE. Statistical analysis was performed using Student's *t*-test or one-way or two-way ANOVA with post hoc comparisons to determine whether the mean of each treatment is different from the untreated cells (control). An α of $P < 0.05$ was considered statistically significant. All statistics were performed using GraphPad Prism version 5 (GraphPad, San Diego, CA).

RESULTS

LPS causes a decrease in $[Zn]_i$ as measured by microspectrofluorimetry in live SPAECs. SPAECs were exposed to LPS or TPEN for 4 h and monitored for changes in FluoZin-3 fluorescence intensity as an index of labile zinc using live cell epifluorescence microscopy. A typical example of such images at 4 h posttreatment is shown in Fig. 1. Compared with control

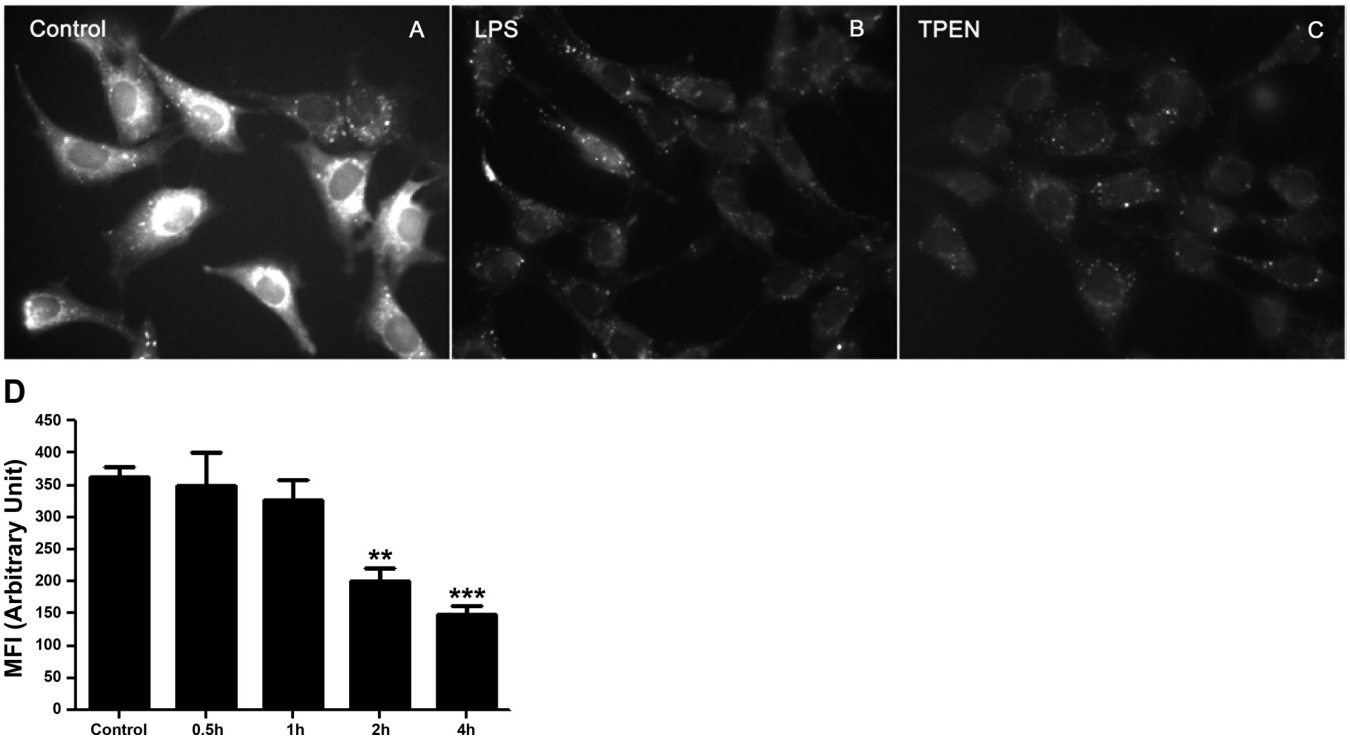

Fig. 1. Effect of LPS on intracellular labile Zn in live sheep pulmonary artery endothelial cells (SPAEC) as determined by microspectrofluorimetry. SPAECs were control (*A*) or treated with LPS (100 ng/ml) (*B*) or N,N,N′,N′-tetrakis(2-pyridylmethyl)ethylenediamine (TPEN) (2 μM) (*C*) for 4 h. Cells were loaded with 5 μM FluoZin-3 AM and equal volume of Pluronic F-127 and imaged by epifluorescence microscope. The images represent fluorescence intensity of FluoZin-3-Zn complex in SPAECs. All images were captured with identical gain, 100% light intensity, 1-ms light exposure and 4 × 4 binning. *D*: time-dependent LPS-induced changes in FluoZin-3 fluorescence in live SPAEC. SPAECs were treated with HBSS (Ca^{2+}/Mg^{2+}) in the presence of LPS (100 ng/ml) for 30 min, 1 h, 2 h, and 4 h, respectively. Control cells received HBSS (Ca^{2+}/Mg^{2+}) in the absence of LPS for 4 h. The data represent means ± SE of mean fluorescence intensity (MFI) of 330–400 randomly selected cells from 5 experiments for each time point. Images were captured using identical gain and camera settings. For analysis of images, background illumination was subtracted from the readings. $^{**}P < 0.01$ and $^{***}P < 0.001$, compared with control; 1-way ANOVA-Tukey.

(Fig. 1*A*), LPS decreased overall fluorescence as shown in Fig. 1*B*. As previously noted (5), FluoZin-3 reports labile or TPEN-sensitive zinc (Fig. 1*C*). SPAECs were exposed to LPS for up to 4 h, and relative changes in mean fluorescence intensity of FluoZin-3 revealed a time-dependent decrease in $[Zn]_i$ as shown in Fig. 1*D*. There was no significant change in overall relative fluorescence at either 0.5 or 1.0 h post-LPS, and then a significant decrease in $[Zn]_i$ was observed at 2 and 4 h of LPS treatment (Fig. 1*D*, 330–400 cells per time point from 5 independent experiments).

LPS causes a decrease in $[Zn]_i$ as determined by flow cytometry. To confirm LPS-induced changes in $[Zn]_i$ in larger sample size, we used FACS to determine relative changes in FluoZin-3 fluorescence for 10,000 cells at each time point (0.5 to 4.0 h) on three different occasions. Representative histograms of cell number vs. relative fluorescence are shown for one such subculture of SPAEC treated with LPS (Fig. 2*A*). The MFI is calculated for the three experiments at each time point and reported in Fig. 2*B*. In agreement with the imaging data shown in Fig. 1, the FACS data (Fig. 2*A*) showed a time-dependent leftward shift in MFI, indicative of an LPS-induced decrease in $[Zn]_i$. During the 4-h period of this experiment, cell viability was >93% (data not shown) as ascertained by PI in either control or LPS-treated SPAEC. Although it appears that a somewhat earlier decrease in $[Zn]_i$ was apparent by FACS (Fig. 2*B*) vs. live cell imaging (Fig. 1*D*), an additional time delay in FACS (e.g., trypsinizing, centrifugation, injection on FACS) makes direct temporal comparison between the two methods challenging.

LPS decreased $[Zn]_i$, as revealed by activity of a zinc-sensitive genetically encoded chimeric reporter. As an alternative to fluorescence detection of changes in $[Zn]_i$, we used a genetic approach and monitored the activity of a highly selective zinc-sensitive chimera (9). SPAECs were transiently cotransfected with pLuc-MCS/MRE and pSVβ-galactosidase. The former plasmid expresses the reporter gene luciferase under the control of tandem repeats of the exclusively zinc-sensitive MREs. β-Galactosidase activity was measured to account for any differences in transfection efficiency. As shown in Fig. 3*A*, there was a significant decrease in relative luciferase activity in SPAEC exposed to LPS for 4 h. As was noted above in fluorescence-based experiments, cell viability (as determined by Alamar Blue) was >92% in cells transfected with above plasmids with or without addition of LPS (Fig. 3*B*).

LPS (and decreases in $[Zn]_i$) upregulates SLC39A14 (ZIP14) mRNA expression. We surveyed the effect of LPS on steady-state mRNA of several representative zinc transporters (ZnT 1, 4, and 6) and importers (ZIP 6, 8, 10, and 14). Using real-time PCR, in two subcultures of SPAEC (one of which is shown in Fig. 4*A*), we noted detectable levels of all of three transporters and four importers. Only ZIP14 appeared to be affected by 4 h of LPS (Fig. 4*A*), and accordingly we expanded our studies on ZIP14 or SLC39A14. We noted that ZIP14 expression (normalized to the housekeeping gene, G6PD) was

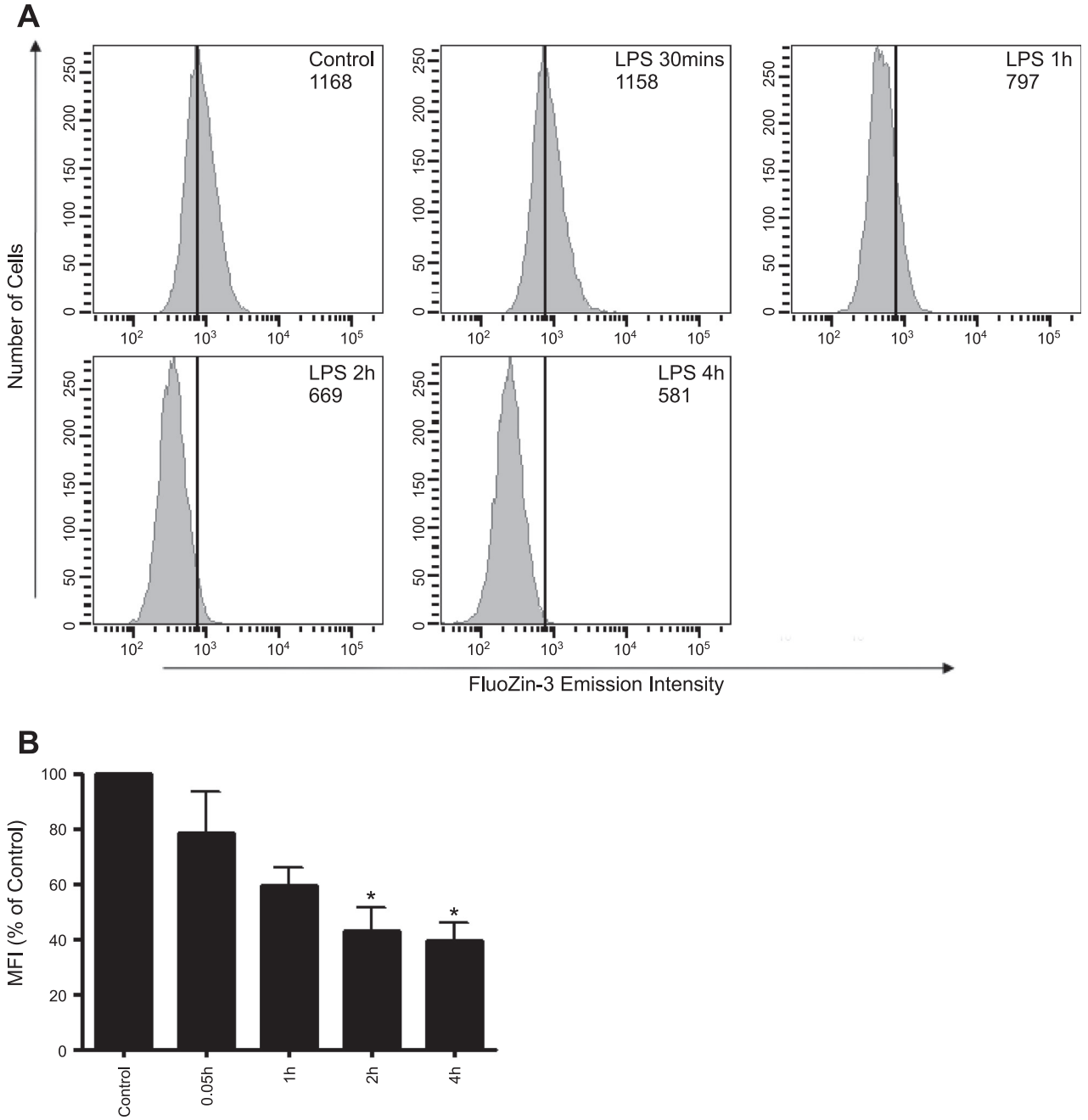

Fig. 2. *A*: typical histograms of subcultures of SPAEC treated with LPS for up to 4 h. SPAECs were treated with HBSS (Ca^{2+}/Mg^{2+}) in the presence of LPS (100 ng/ml) for 30 min, 1 h, 2 h, and 4 h, respectively. Control cells received HBSS (Ca^{2+}/Mg^{2+}) in the absence of LPS for 4 h. Data demonstrate the histogram of MFI of 10,000 cells for each time point. The histograms are representative of 1 subculture of SPAEC treated with LPS. Numbers in each histogram indicate MFI. *B*: bar graph represents means ± SE of MFI (% of control) of samples measured in triplicate for 3 independent experiments. *$P < 0.01$ compared with control; 1-way ANOVA-Tukey.

not affected by exogenous zinc (in the presence of the zinc ionophore, pyrithione) but was increased approximately fivefold by LPS (Fig. 4*B*). The effect of LPS was abolished by the addition of exogenous zinc (Fig. 4*B*), suggesting that LPS-induced increases in ZIP14 mRNA may be secondary to the decreases in $[Zn]_i$ as shown above (Figs. 1–3). This was supported by the sensitivity of ZIP14 mRNA to TPEN, an effect, in itself, that was reversible with exogenous zinc (Fig. 4*C*). Indeed TPEN could augment the effect of LPS on increases in ZIP14 mRNA when administered simultaneously (data not shown).

LPS initiates apoptosis via an intrinsic mitochondria-dependent pathway. We previously (25) reported that 100 ng/ml LPS caused DNA damage at 4 h in SPAEC as revealed by nuclear morphology, in situ labeling by break extension, and internucleosomal DNA fragmentation. To confirm that LPS caused apoptosis in SPAEC, we used FACS analysis of annexin-V binding and showed (Fig. 5*A*) that there was a time-dependent increase in

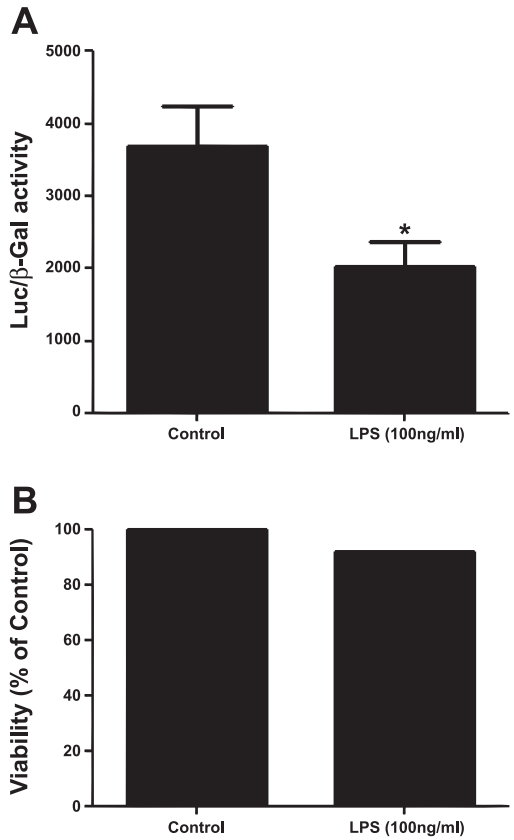

Fig. 3. *A*: LPS decreases expression of a chimeric zinc-sensitive reporter. SPAECs were transiently cotransfected with pLuc-MCS/4MREa (0.6 μg) and pSVβ-galactosidase (0.15 μg). 24 h after transfection, cells were treated with or without LPS (100 ng/ml) for 4 h in the presence of serum (10%) and subsequently assayed for luciferase and β-galactosidase (β-Gal) activity 4 h posttreatment. A significant decrease in luciferase activity was observed in LPS-stimulated cells with viability greater than 92%. Luciferase activity is expressed as a ratio of firefly luciferase (pLucMRE) activity to β-galactosidase activity. Data represent means ± SE of luciferase activity of samples measured in triplicate for 9 independent experiments (*$P < 0.05$; independent, two-tailed *t*-test). *B*: cell viability was assessed by Alamar Blue. Alamar Blue fluorescence was measured as an index of viability 4 h post-LPS treatment. Data represent Alamar Blue fluorescence (% of control) measured in triplicate.

annexin-V-positive (and PI-negative) SPAEC over 24 h. LPS-induced annexin-V binding was sensitive to Z-VAD, a pan-caspase inhibitor, from 4–24 h, consistent with a process of apoptosis (Fig. 5*A*). This process appeared to be intrinsic mitochondria-dependent because cytosolic cytochrome increased in a time-dependent fashion after LPS (Fig. 5*B*). Accordingly, we studied the effects of $[Zn]_i$ on early (4 h) aspects (e.g., caspase-3/7 activation, see below) of LPS-induced apoptosis in SPAEC.

LPS-induced decreases in $[Zn]_i$ contribute to apoptosis in SPAEC. As previously reported (23–25), acute treatment (4 h) with LPS did not affect cell viability as determined by Alamar

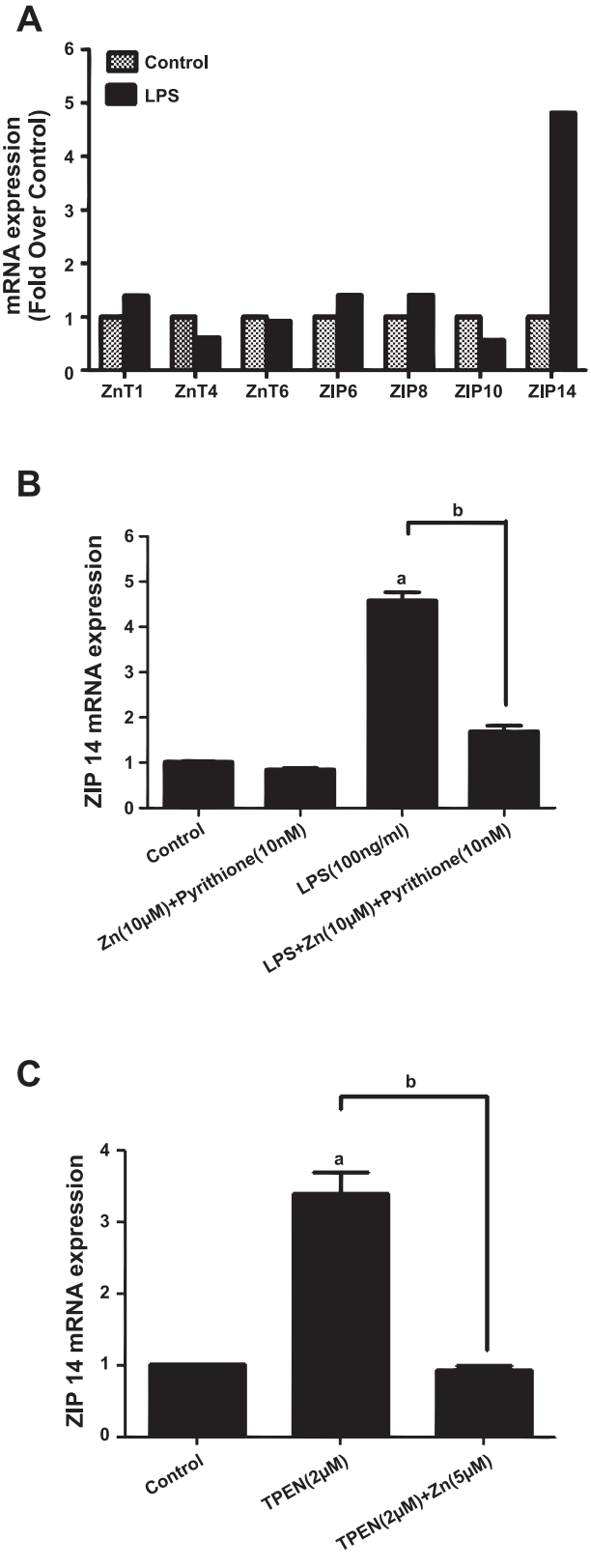

Fig. 4. Effect of LPS and decreased $[Zn]_i$ on representative zinc transporters and importers. SPAECs were exposed to LPS (100 ng/ml) or HBSS (Ca^{2+}/Mg^{2+}) for 4 h. Total RNA was isolated and ZnT 1, 4, and 6 and ZIP 6, 8, 10, and 14 mRNA levels were measured by real-time PCR using specific primers and normalized to the housekeeping gene glucose-6-phosphate dehydrogenase (G6PD). *A*: representative of 1 of 2 subcultures analyzed in triplicate. *B*: effect of LPS (and its reversibility with exogenous zinc) on ZIP14 mRNA. Values are means ± SE of mRNA expression of samples measured in triplicate for 4 separate subcultures. *C*: effect of TPEN (and its reversibility with exogenous zinc) on ZIP14 mRNA. Values are means ± SE of mRNA expression of samples measured in triplicate for 4 separate subcultures ($^aP < 0.001$ compared with control; $^bP < 0.001$ compared with LPS and TPEN treatment, respectively; 1-way ANOVA-Tukey).

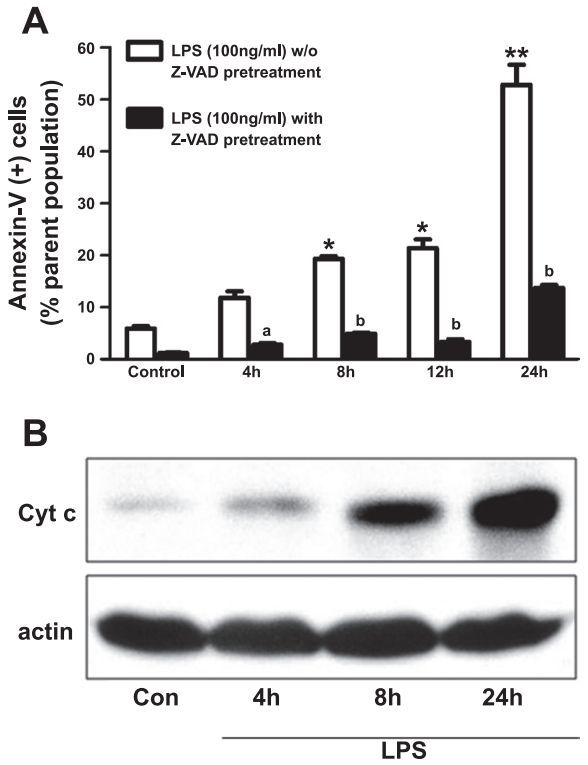

Fig. 5. LPS causes intrinsic mitochondria-dependent apoptosis in SPAEC. *A*: LPS causes a time-dependent Z-Val-Ala-Asp (Z-VAD)-sensitive increase in annexin-V binding in SPAEC. SPAECs were treated with LPS (100 ng/ml) in HBSS (Ca^{2+}/Mg^{2+}) for 4, 8, 12, and 24 h. Control cells received HBSS (Ca^{2+}/Mg^{2+}) for 24 h. Apoptosis was determined by measuring phosphatidylserine (PS) externalization (by annexin-V labeling) and reported as PS-positive, propidium iodide-negative percentage of total cell population (via fluorescence-activated cell sorting). 4 experiments were performed on 2 subcultures, and values are means ± SE. $*P < 0.01$ and $**P < 0.001$ compared with control, respectively; $^{a}P < 0.05$ and $^{b}P < 0.001$ compared with without Z-VAD pretreatment. Comparisons were made with two-way ANOVA-Bonferroni. B: LPS mediates cytochrome *c* (cyt *c*) release in cytosol of SPAEC. 1 subculture of SPAEC was exposed to LPS (100 ng/ml) for 4, 8, and 24 h in HBSS (Ca^{2+}/Mg^{2+}). Control cells received HBSS (Ca^{2+}/Mg^{2+}) for 24 h. Total protein was isolated, and cyt *c* and β-actin level were determined by Western blot analysis.

Blue (Fig. 6*A* or PI, data not shown), In Fig. 6*B*, we note that LPS caused a significant increase in caspase-3/7 activity at 4 h. Although zinc (in the presence of pyrithione), by itself, did not affect caspase-3/7 activity, it did rescue the effect of LPS on caspase-3/7 activity, consistent with our hypothesis that decreases in $[Zn]_i$ contributed to LPS-mediated apoptosis. This was further confirmed by noting that a concentration of TPEN (2 μM) sufficient to greatly reduce $[Zn]_i$ as ascertained by FluoZin-3 (Fig. 1*C*) was sufficient to cause comparable increases to LPS in caspase-3/7 activity, and the effect of TPEN was sensitive to exogenous zinc (Fig. 6*C*). We (44) previously

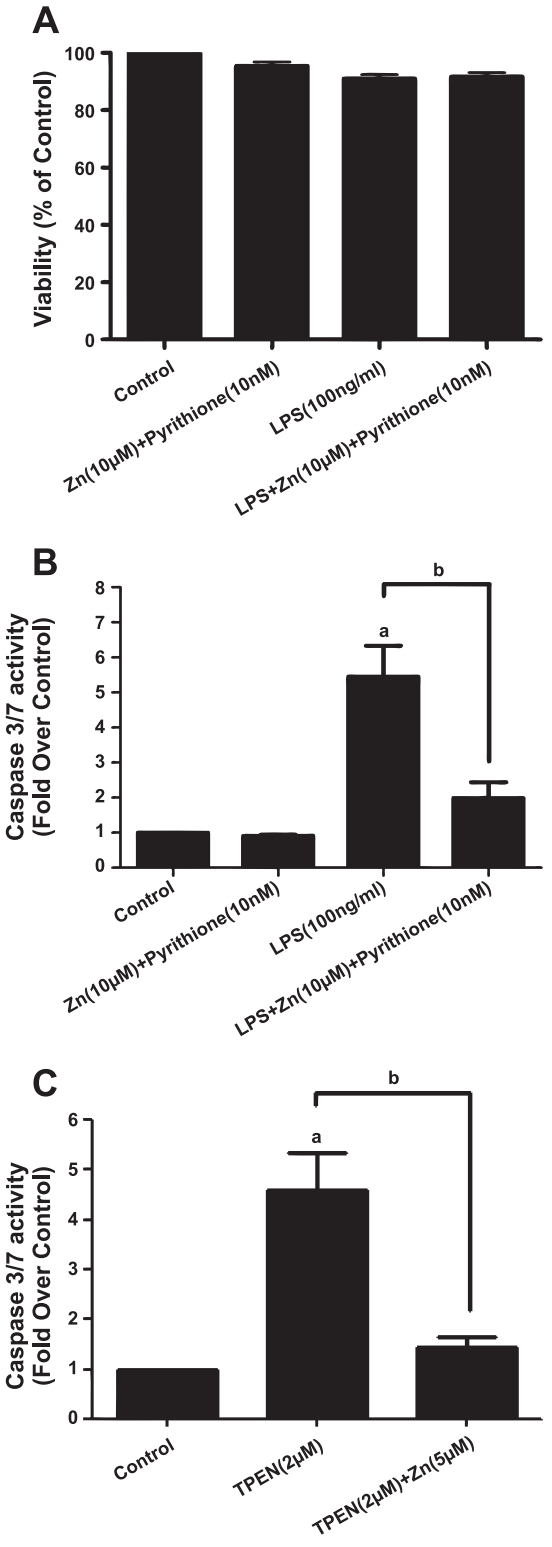

Fig. 6. LPS activates caspase-3/7 in a zinc-dependent fashion. *A*: lack of effect of LPS (or exogenous zinc) on cell viability in SPAEC. Cell viability was assessed by Alamar Blue. Data represent means ± SE of Alamar Blue fluorescence (% of control) of samples measured in triplicate for 4 independent experiments. *B*: LPS activates caspase-3/7 in SPAEC. SPAECs were treated with LPS (100 ng/ml) or HBSS (Ca^{2+}/Mg^{2+}) for 4 h, and caspase-3/7 activity was measured as described. Data represent means ± SE of caspase-3/7 activity (fold over control) of samples measured in triplicate for 4 independent experiments. *C*: zinc chelation activates caspase-3/7 activity in SPAEC. SPAEC were treated with TPEN (2 μM) with and without 5 μM zinc added to medium for 4 h, and caspase-3/7 activity was measured as described. Data represent means ± SE of caspase-3/7 activity (fold over control) of samples measured in triplicate for 4 independent experiments. $^{a}P < 0.001$ compared with control; $^{b}P < 0.01$ compared with LPS treatment (*B*) or TPEN (*C*) by 1-way ANOVA-Tukey.

ascribed such a TPEN-sensitive effect to a process of apoptosis in SPAEC.

DISCUSSION

To examine the function of zinc homeostasis in pulmonary endothelial cell apoptosis, we exposed SPAECs to LPS (100 ng/ml) for 4 h and then monitored changes in $[Zn]_i$ by chemical (labile zinc fluorophore, FluoZin-3) and genetic approaches (zinc-sensitive chimeric reporter and ZIP14 mRNA) assays. Epifluorescence microscopy (Fig. 1) revealed that LPS causes a decrease in $[Zn]_i$ in live cells that was significant at 2 h. This was confirmed in a larger number of cells by complementary methodology of flow cytometry (Fig. 2). Additional confirmation of LPS-induced decreases in $[Zn]_i$ was achieved by nonchemical genetic approaches (Figs. 3 and 4). The functional significance of LPS-induced decreases in $[Zn]_i$ was revealed by the ability of exogenous zinc to rescue LPS-induced activation of caspase-3/7 (Fig. 6*B*).

Labile $[Zn]_i$ and signal transduction. The role of labile $[Zn]_i$ in signal transduction is an emerging area in cell biology (21, 22, 8) and is fostered in part by *1*) intricacies of zinc homeostasis including a large family of importers, transporters and binding proteins (34); *2*) extraordinary large number of potential regulatory targets [~3–10% of genome; (1)]; *3*) association of chronic (and rare) disorders with altered zinc homeostasis secondary to mutations/variants in zinc importers and transporters and/or interactions with altered zinc nutritional status (15); and *4*) facileness of inorganic chemistry and coordination dynamics of zinc in affecting protein function (6). Major limitations in the field are the lack of *1*) readily available fluorophores that are quantitative as well as specific for putative labile $[Zn]_i$ (28, 29) and *2*) zinc-specific chemical chelators. Although progress has been made in both these areas (53), many studies define labile $[Zn]_i$ as that compartment that can alter relative fluorescence of a variety of zinc-sensitive fluorophores (including FluoZin-3) and is sensitive to chelation by membrane-permeant compounds such as TPEN. In this regard, advantageous features of FluoZin-3 include its selectivity (K_d = 15 nM) for zinc (e.g., magnesium, calcium, and iron do not bind to the dye at concentrations well above what these cations may reach inside mammalian cells) (14, 57). Binding of FluoZin-3 to labile zinc is unaffected by low intracellular pH or oxidants (14, 27). Nonetheless, it is a nonratiometric dye, and thus issues of loading, bleaching, and lack of quantitative calibration persist. Furthermore, as with all detectors of this nature, one has to introduce a potential new buffer (of zinc). As such, we took extra steps to confirm relative changes using microscopy (Fig. 1) and FACS (Fig. 2; to recruit large number of cells) as well as genetic (Fig. 3: pLucMSC/MRE; Fig. 4: mRNA ZIP14) to increase our confidence that LPS caused a decrease in $[Zn]_i$.

LPS and $[Zn]_i$. Most studies examining a signal transduction role for labile $[Zn]_i$ followed the paradigm of calcium homeostasis, the other major intracellular nonredox active divalent cation, and looked for rapid and large increases secondary to extracellular flux or more often attributable to release from intracellular stores (54). In the case of LPS-treated pulmonary endothelial cells, we initially (44) did not detect changes in labile $[Zn]_i$ 30 min post-LPS treatment. In the present study, there were no changes up to 2 h (Fig. 1). Haase et al. (20) did detect increases in labile $[Zn]_i$ 30 min post-LPS in human monocytes and granulocytes, but not lymphocytes. In this same report, they noted even earlier increases (within 2 min) in the murine macrophage cell line. Nonetheless, like the original report of Kitamura et al. (30), who detected decreases in labile $[Zn]_i$ 6 h after treating mouse dendritic cells with LPS, we noted relative delayed decreases in labile $[Zn]_i$ at 2–4 h in SPAEC. This delayed effect was not likely attributable to artifacts of FluoZin-3 because it was reproducible with MRE-Luc chimera (Fig. 3), and we suggest it may be important for the signaling events associated with cell death and apoptosis. The mechanism underlying this delayed LPS-mediated decrease in labile $[Zn]_i$ remains unclear. It is possible that an imbalance attributable to changes in members of ZnT or ZIP families might underlie our observations, but we did not detect LPS-induced increases in mRNA in the former or decreases in the latter group, respectively. Indeed, it appears that ZIP14 mRNA increased (Fig. 4, *A* and *B*), presumably secondary to a decrease in labile zinc (as it was mimicked by TPEN, Fig. 4*C*), suggesting a possible important feedback loop in which ZIP14 expression (perhaps via zinc-sensitive promoter regions) is modulated to maintain $[Zn]_i$ homeostasis. Present available information on regulation of Zip14 expression (19) is limited to the role of IL-6 (34) and IL-1 (35) in hepatocytes with an obligatory contribution of NO signaling (via action potential-1) affecting ZIP14 expression. We did not examine the potential of such autocrine effects to LPS in our system. It is possible that LPS affected ZnT or ZIP family members at a posttranslational level, but the limited availability of antibodies and the lack of electrophysiological assessment of zinc transport make such studies challenging.

Zinc and cell death. Zinc has been a primary antiapoptotic molecule since the process of apoptosis was described (10). Subsequently earlier and more subtle zinc-sensitive targets including caspase-3 (40) and poly(ADP-ribose)polymerase (43) emerged as candidates for such antiapoptotic activity of zinc. A detailed examination in HL60 cells by Duffy et al. (16) provided convincing evidence that decreases in intracellular zinc preceded early indicators of apoptosis in transformed human promyelocytic cell (HL60). We (44) and Virag et al. (50) both concluded that high levels of intracellular zinc contributed to necrosis and that low levels were proapoptotic. Nonetheless, in dendritic cells, modest (<100 μM) levels of exogenous zinc activated acid sphingomyelinase, leading to production of ceramide and apoptotic cell death (1). In fetal SPAEC, hydrogen peroxide-induced increases in zinc were associated with apoptosis, and this effect was blunted by zinc chelators including TPEN or overexpression of metallothionein (51). This suggests that some effects of zinc and apoptosis are cell specific and/or dependent on developmental stage. As has been shown in systemic endothelium using different proapoptotic stimuli (7), in LPS-treated SPAEC, TPEN exacerbates apoptosis (44) and exogenous zinc can rescue this phenotype (Fig. 6*B*). In the more complex scenario in which NO is introduced into the milieu of LPS-treated SPAEC, we (45) noted that NO-mediated resistance to LPS was Zn dependent, suggesting that elevations in labile $[Zn]_i$ secondary to either influx from extracellular sources or chemically mediated release of zinc, perhaps from metallothionein (42), can produce LPS-resistant phenotypes.

Zinc and acute lung injury. Zinc deficiencies increase the susceptibility of experimental animals to hyperoxic (46), alcohol-induced (26), and sepsis-induced (31) lung injury. We (32) and others (56) have reviewed the role of zinc in acute lung injury, and the majority of our insight is related to airway epithelium (6, 47, 48). The proximity of a labile pool of zinc and procaspase-3 in ciliary basal bodies of airway epithelium and the ability of TPEN to cause apoptosis or exacerbate other proapoptotic stimuli provided support for an antiapoptotic role of labile zinc (8, 18, 49) in airway epithelium. Further details of an antiapoptotic role for zinc in human airway epithelium were provided by Bao and Knoell (2, 3), who reported that zinc depletion exacerbated apoptosis and decreased barrier function secondary to Fas antibody, TNF-α, and IFN-γ. These authors extended these studies to show that zinc depletion augmented acute lung injury (including apoptosis, enhanced inflammation, altered innate immunity) in polymicrobial sepsis in mice (4, 31). Collectively, these reports underscore the importance of zinc metabolism in the airway and lung and suggest that zinc supplementation may be of therapeutic utility, and further insights into zinc homeostasis may reveal critical aspects of pathogenesis in acute and chronic lung disorders (55).

Our findings show for the first time that a decrease in labile zinc in pulmonary endothelium is an important signaling event in LPS-induced apoptosis. Along with the report of Kitamura et al. (30), it suggests that such a change in labile $[Zn]_i$ may be an important mechanism by which cells respond to exogenous stimuli such as LPS. Critical future efforts should be directed toward understanding the mechanism by which $[Zn]_i$ decreases, the cellular targets affected by such a decrease, and the overall physiological processes (in addition to apoptosis) that occur in the setting of LPS and pulmonary endothelium.

ACKNOWLEDGMENTS

The authors thank Dr. Giegroc for providing the pLuc-MCS/4MREa reporter construct and Dr. Nemec (Yale University), Dr. Dalrymple (CSIRO Livestock Industries), and Ms. Linda Klei (University of Pittsburgh) for contribution in this work.

GRANTS

This work was supported by NIH R37 HL65697 (B. Pitt), NIH R01 HL081421 (C. St. Croix), NIH HL 70755, and a predoctoral fellowship from the American Heart Association (K. Thambiayya).

DISCLOSURES

No conflicts of interest, financial or otherwise are declared by the authors.

REFERENCES

1. **Andreini C, Banci L, Bertini I, Rosato A.** Zinc through the three domains of life. *J Proteome Res* 5: 3173–3178, 2006.
2. **Bao S, Knoell DL.** Zinc modulates airway epithelium susceptibility to death receptor-mediated apoptosis. *Am J Physiol Lung Cell Mol Physiol* 290: L433–L441, 2006.
3. **Bao S, Knoell DL.** Zinc modulates cytokine-induced lung epithelial cell barrier permeability. *Am J Physiol Lung Cell Mol Physiol* 291: L1132–L1141, 2006.
4. **Bao S, Liu MJ, Lee B, Besecker B, Lai JP, Guttridge DC, Knoell DL.** Zinc modulates the innate immune response in vivo to polymicrobial sepsis through regulation of NF-κB. *Am J Physiol Lung Cell Mol Physiol* 298: L744–L754, 2010.
5. **Bernal PJ, Leelavanichkul K, Bauer E, Cao R, Wilson A, Wasserloos KJ, Watkins SC, Pitt BR, St Croix CM.** Nitric-oxide-mediated zinc release contributes to hypoxic regulation of pulmonary vascular tone. *Circ Res* 102: 1575–1583, 2008.
6. **Besecker B, Bao S, Bohacova B, Papp A, Sadee W, Knoell DL.** The human zinc transporter SLC39A8 (Zip8) is critical in zinc-mediated cytoprotection in lung epithelia. *Am J Physiol Lung Cell Mol Physiol* 294: L1127–L1136, 2008.
7. **Bozym RA, Thompson RB, Stoddard AK, Fierke CA.** Measuring picomolar intracellular exchangeable zinc in PC-12 cells using a ratiometric fluorescence biosensor. *ACS Chem Biol* 1: 103–111, 2006.
8. **Carter JE, Truong-Tran AQ, Grosser D, Ho L, Ruffin RE, Zalewski PD.** Involvement of redox events in caspase activation in zinc-depleted airway epithelial cells. *Biochem Biophys Res Commun* 297: 1062–1070, 2002.
9. **Chen X, Zhang B, Harmon PM, Schaffner W, Peterson DO, Giedroc DP.** A novel cysteine cluster in human metal-responsive transcription factor 1 is required for heavy metal-induced transcriptional activation in vivo. *J Biol Chem* 279: 4515–4522, 2004.
10. **Cohen JJ, Duke RC.** Glucocorticoid activation of a calcium-dependent endonuclease in thymocyte nuclei leads to cell death. *J Immunol* 132: 38–42, 1984.
11. **Colvin RA, Bush AI, Volitakis I, Fontaine CP, Thomas D, Kikuchi K, Holmes WR.** Insights into Zn2+ homeostasis in neurons from experimental and modeling studies. *Am J Physiol Cell Physiol* 294: C726–C742, 2008.
12. **Cousins RJ, Liuzzi JP, Lichten LA.** Mammalian zinc transport, trafficking, and signals. *J Biol Chem* 281: 24085–24089, 2006.
13. **Dalrymple BP, Kirkness EF, Nefedov M, McWilliam S, Ratnakumar A, Barris W, Zhao S, Shetty J, Maddox JF, O'Grady M, Nicholas F, Crawford AM, Smith T, de Jong PJ, McEwan J, Oddy VH, Cockett NE.** Using comparative genomics to reorder the human genome sequence into a virtual sheep genome (Abstract). *Genome Biol* 8: R152, 2007.
14. **Devinney MJ 2nd, Reynolds IJ, Dineley KE.** Simultaneous detection of intracellular free calcium and zinc using fura-2FF and FluoZin-3. *Cell Calcium* 37: 225–232, 2005.
15. **Devirgiliis C, Zalewski PD, Perozzi G, Murgia C.** Zinc fluxes and zinc transporter genes in chronic diseases. *Mutat Res* 622: 84–93, 2007.
16. **Duffy JY, Miller CM, Rutschilling GL, Ridder GM, Clegg MS, Keen CL, Daston GP.** A decrease in intracellular zinc level precedes the detection of early indicators of apoptosis in HL-60 cells. *Apoptosis* 6: 161–172, 2001.
17. **Eide DJ.** The SLC39 family of metal ion transporters. *Pflügers Arch* 447: 796–800, 2004.
18. **Fanzo JC, Reaves SK, Cui L, Zhu L, Wu JY, Wang YR, Lei KY.** Zinc status affects p53, gadd45, and c-fos expression and caspase-3 activity in human bronchial epithelial cells. *Am J Physiol Cell Physiol* 281: C751–C757, 2001.
19. **Girijashanker K, He L, Soleimani M, Reed JM, Li H, Liu Z, Wang B, Dalton TP, Nebert DW.** Slc39a14 gene encodes ZIP14, a metal/bicarbonate symporter: similarities to the ZIP8 transporter. *Mol Pharmacol* 73: 1413–1423, 2008.
20. **Haase H, Ober-Blobaum JL, Engelhardt G, Hebel S, Heit A, Heine H, Rink L.** Zinc signals are essential for lipopolysaccharide-induced signal transduction in monocytes. *J Immunol* 181: 6491–6502, 2008.
21. **Haase H, Rink L.** Functional significance of zinc-related signaling pathways in immune cells. *Annu Rev Nutr* 29: 133–152, 2009.
22. **Haase H, Rink L.** The immune system and the impact of zinc during aging (Abstract). *Immun Ageing* 6: 9, 2009.
23. **Hoyt DG, Mannix RJ, Gerritsen ME, Watkins SC, Lazo JS, Pitt BR.** Integrins inhibit LPS-induced DNA strand breakage in cultured lung endothelial cells. *Am J Physiol Lung Cell Mol Physiol* 270: L689–L694, 1996.
24. **Hoyt DG, Mannix RJ, Rusnak JM, Pitt BR, Lazo JS.** Collagen is a survival factor against LPS-induced apoptosis in cultured sheep pulmonary artery endothelial cells. *Am J Physiol Lung Cell Mol Physiol* 269: L171–L177, 1995.
25. **Hoyt DG, Rizzo M, Gerritsen ME, Pitt BR, Lazo JS.** Integrin activation protects pulmonary endothelial cells from the genotoxic effects of bleomycin. *Am J Physiol Lung Cell Mol Physiol* 273: L612–L617, 1997.
26. **Joshi PC, Mehta A, Jabber WS, Fan X, Guidot DM.** Zinc deficiency mediates alcohol-induced alveolar epithelial and macrophage dysfunction in rats. *Am J Respir Cell Mol Biol* 41: 207–216, 2009.
27. **Kay AR.** Evidence for chelatable zinc in the extracellular space of the hippocampus, but little evidence for synaptic release of Zn. *J Neurosci* 23: 6847–6855, 2003.
28. **Kikuchi K, Komatsu K, Nagano T.** Zinc sensing for cellular application. *Curr Opin Chem Biol* 8: 182–191, 2004.

29. **Kimura E, Aoki S.** Chemistry of zinc(II) fluorophore sensors. *Biometals* 14: 191–204, 2001.
30. **Kitamura H, Morikawa H, Kamon H, Iguchi M, Hojyo S, Fukada T, Yamashita S, Kaisho T, Akira S, Murakami M, Hirano T.** Toll-like receptor-mediated regulation of zinc homeostasis influences dendritic cell function. *Nat Immunol* 7: 971–977, 2006.
31. **Knoell DL, Julian MW, Bao S, Besecker B, Macre JE, Leikauf GD, DiSilvestro RA, Crouser ED.** Zinc deficiency increases organ damage and mortality in a murine model of polymicrobial sepsis. *Crit Care Med* 37: 1380–1388, 2009.
32. **Li H, Cao R, Wasserloos KJ, Bernal P, Liu ZQ, Pitt BR, St Croix CM.** Nitric oxide and zinc homeostasis in pulmonary endothelium. *Ann NY Acad Sci* 1203: 73–78, 2010.
33. **Li Y, Maret W.** Transient fluctuations of intracellular zinc ions in cell proliferation. *Exp Cell Res* 315: 2463–2470, 2009.
34. **Lichten LA, Cousins RJ.** Mammalian zinc transporters: nutritional and physiologic regulation. *Annu Rev Nutr* 29: 153–176, 2009.
35. **Lichten LA, Liuzzi JP, Cousins RJ.** Interleukin-1β contributes via NO to the upregulation and functional activity of the zinc transporter Zip14 (Slc39a14) in murine hepatocytes. *Am J Physiol Gastrointest Liver Physiol* 296: G860–G867, 2009.
36. **Maret W, Li Y.** Coordination dynamics of zinc in proteins. *Chem Rev* 109: 4682–4707, 2009.
37. **Meerarani P, Ramadass P, Toborek M, Bauer HC, Bauer H, Hennig B.** Zinc protects against apoptosis of endothelial cells induced by linoleic acid and tumor necrosis factor alpha. *Am J Clin Nutr* 71: 81–87, 2000.
38. **Murakami M, Hirano T.** Intracellular zinc homeostasis and zinc signaling. *Cancer Sci* 99: 1515–1522, 2008.
39. **Nemec AA, Leikauf GD, Pitt BR, Wasserloos KJ, Barchowsky A.** Nickel mobilizes intracellular zinc to induce metallothionein in human airway epithelial cells. *Am J Respir Cell Mol Biol* 41: 69–75, 2009.
40. **Perry DK, Smyth MJ, Stennicke HR, Salvesen GS, Duriez P, Poirier GG, Hannun YA.** Zinc is a potent inhibitor of the apoptotic protease, caspase-3. A novel target for zinc in the inhibition of apoptosis. *J Biol Chem* 272: 18530–18533, 1997.
41. **Shumilina E, Xuan NT, Schmid E, Bhavsar SK, Szteyn K, Gu S, Gotz F, Lang F.** Zinc induced apoptotic death of mouse dendritic cells. *Apoptosis* 15: 1177–1186, 2010.
42. **St Croix CM, Wasserloos KJ, Dineley KE, Reynolds IJ, Levitan ES, Pitt BR.** Nitric oxide-induced changes in intracellular zinc homeostasis are mediated by metallothionein/thionein. *Am J Physiol Lung Cell Mol Physiol* 282: L185–L192, 2002.
43. **Takahashi A, Alnemri ES, Lazebnik YA, Fernandes-Alnemri T, Litwack G, Moir RD, Goldman RD, Poirier GG, Kaufmann SH, Earnshaw WC.** Cleavage of lamin A by Mch2 alpha but not CPP32: multiple interleukin 1 beta-converting enzyme-related proteases with distinct substrate recognition properties are active in apoptosis. *Proc Natl Acad Sci USA* 93: 8395–8400, 1996.
44. **Tang ZL, Wasserloos K, St Croix CM, Pitt BR.** Role of zinc in pulmonary endothelial cell response to oxidative stress. *Am J Physiol Lung Cell Mol Physiol* 281: L243–L249, 2001.
45. **Tang ZL, Wasserloos KJ, Liu X, Stitt MS, Reynolds IJ, Pitt BR, St Croix CM.** Nitric oxide decreases the sensitivity of pulmonary endothelial cells to LPS-induced apoptosis in a zinc-dependent fashion. *Mol Cell Biochem* 234–235: 211–217, 2002.
46. **Taylor CG, Bray TM.** Effect of hyperoxia on oxygen free radical defense enzymes in the lung of zinc-deficient rats. *J Nutr* 121: 460–466, 1991.
47. **Truong-Tran AQ, Carter J, Ruffin R, Zalewski PD.** New insights into the role of zinc in the respiratory epithelium. *Immunol Cell Biol* 79: 170–177, 2001.
48. **Truong-Tran AQ, Carter J, Ruffin RE, Zalewski PD.** The role of zinc in caspase activation and apoptotic cell death. *Biometals* 14: 315–330, 2001.
49. **Truong-Tran AQ, Ruffin RE, Zalewski PD.** Visualization of labile zinc and its role in apoptosis of primary airway epithelial cells and cell lines. *Am J Physiol Lung Cell Mol Physiol* 279: L1172–L1183, 2000.
50. **Virag L, Szabo C.** Inhibition of poly(ADP-ribose) synthase (PARS) and protection against peroxynitrite-induced cytotoxicity by zinc chelation. *Br J Pharmacol* 126: 769–777, 1999.
51. **Wiseman DA, Wells SM, Hubbard M, Welker JE, Black SM.** Alterations in zinc homeostasis underlie endothelial cell death induced by oxidative stress from acute exposure to hydrogen peroxide. *Am J Physiol Lung Cell Mol Physiol* 292: L165–L177, 2007.
52. **Wiseman DA, Wells SM, Wilham J, Hubbard M, Welker JE, Black SM.** Endothelial response to stress from exogenous Zn2+ resembles that of NO-mediated nitrosative stress, and is protected by MT-1 overexpression. *Am J Physiol Cell Physiol* 291: C555–C568, 2006.
53. **Xu Z, Yoon J, Spring DR.** Fluorescent chemosensors for Zn(2+). *Chem Soc Rev* 39: 1996–2006, 2010.
54. **Yamasaki S, Sakata-Sogawa K, Hasegawa A, Suzuki T, Kabu K, Sato E, Kurosaki T, Yamashita S, Tokunaga M, Nishida K, Hirano T.** Zinc is a novel intracellular second messenger. *J Cell Biol* 177: 637–645, 2007.
55. **Zalewski PD.** Zinc metabolism in the airway: basic mechanisms and drug targets. *Curr Opin Pharmacol* 6: 237–243, 2006.
56. **Zalewski PD, Truong-Tran AQ, Grosser D, Jayaram L, Murgia C, Ruffin RE.** Zinc metabolism in airway epithelium and airway inflammation: basic mechanisms and clinical targets. A review. *Pharmacol Ther* 105: 127–149, 2005.
57. **Zhao J, Bertoglio BA, Gee KR, Kay AR.** The zinc indicator FluoZin-3 is not perturbed significantly by physiological levels of calcium or magnesium. *Cell Calcium* 44: 422–426, 2008.